


**Quantum algorithm for the microcanonical thermal pure quantum state method**Kaito Mizukami and Akihisa Koga *Department of Physics, Tokyo Institute of Technology, Meguro, Tokyo 152-8551, Japan*

(Received 21 September 2022; accepted 13 June 2023; published 6 July 2023)

We propose a quantum algorithm to investigate finite-temperature properties of quantum many-body systems by implementing the microcanonical thermal pure quantum (TPQ) states [S. Sugiura and A. Shimizu, *Phys. Rev. Lett.* **108**, 240401 (2012)] on a quantum computer. In the formalism, the TPQ state is constructed by applying the power of a rescaled Hamiltonian to a random state. We clarify that, using techniques based on quantum signal processing, the power operation can be efficiently realized when the ground-state energy of a quantum system of interest is given with some precision. Our algorithm has an advantage in calculating thermodynamic quantities at low temperatures.

DOI: [10.1103/PhysRevA.108.012404](https://doi.org/10.1103/PhysRevA.108.012404)**I. INTRODUCTION**

Studying thermodynamic properties of quantum many-body systems is of great importance for not only improving the fundamental understanding but also the designing of complex quantum materials in condensed matter physics. However, such systems are often difficult to simulate on classical computers since its Hilbert space grows exponentially with respect to the system size. For example, when the  $S = 1/2$  quantum spin model with the finite system size  $N$  is considered, each quantum state is represented by a vector with  $2^N$  elements, which makes it hard to directly deal with the larger system on classical computers. The quantum Monte Carlo simulation is one of the most powerful methods to treat the large systems since thermodynamic quantities are evaluated by random samplings. However, in frustrated systems, the sign problem appears at low temperatures, making it difficult to investigate thermodynamic properties except for the special cases [1,2]. Therefore, another tool is desired to examine thermodynamic properties in the generic quantum systems with large clusters.

Quantum computers have been considered as potential tools to simulate quantum many-body systems efficiently over classical computers [3]. Hence, exploring finite-temperature properties is one of the important applications of quantum computers. Thermal states at finite temperatures are basically expressed by the density matrices corresponding to thermodynamic ensembles in statistical mechanics, which are the mixed states of pure quantum states. There exist some algorithms that prepare the Gibbs states in accordance with the canonical ensemble by making use of phase estimation [4–7] or variational method [8–10] via some purifications. In this case, thermodynamic quantities can be calculated directly.

On the other hand, it is often computationally efficient to use some random states according to statistical ensembles rather than using the thermal density matrices. One example is the Monte Carlo sampling method using a quantum computer [11–15], which circumvents the sign problem. However, the calculations for large systems require more resources as estimating thermal averages generally requires a large number

of samples with increasing the system size. Another complementary method is the thermal pure quantum (TPQ) state method [16,17]. In this method, one starts with a random state that corresponds to the state at infinite temperature limit. Applying an appropriate Hermitian operator according to the desired ensemble to the initial state, one obtains a TPQ state, which is a pure quantum state representing an equilibrium state [16,17]. Remarkably, the TPQ states allow for efficient calculation of thermodynamic quantities with a small number of samples.

Recently, some applications of the canonical TPQ state corresponding to the canonical ensemble, which is formed by the imaginary time evolution (ITE), to quantum computation have been proposed [18,19] using a quantum ITE algorithm [14], Suzuki-Trotter decomposition [20], or polynomial expansion [21]. On the other hand, in order to explore thermodynamic properties in isolated systems, e.g., the effects of the disorders and real-time dynamics in finite systems, the microcanonical TPQ states corresponding to the microcanonical ensemble should be important. In this formalism [16], the TPQ state is obtained by iteratively applying a properly rescaled Hamiltonian, i.e., by multiplying the power of the rescaled Hamiltonian to a random state. It is known that, even in small clusters that are available on classical computers, the microcanonical TPQ state method reasonably describes finite-temperature properties in the thermodynamic limit as it has recently been applied to interesting systems such as the Heisenberg model on frustrated lattices [16,17,22–26] and the Kitaev models [27–34] with a classical computer. While a hybrid quantum-classical algorithm for a different microcanonical TPQ state with specified energy has been proposed recently [35], it is also instructive to construct the original microcanonical TPQ states by means of a quantum algorithm.

The paper presents a quantum algorithm for the microcanonical TPQ state method [16]. In our scheme, multiple products of the rescaled Hamiltonian for constructing the TPQ states are realized by taking advantage of some techniques based on quantum signal processing (QSP) [36,37]. Specifically, we employ three techniques called the block encoding [38,39], quantum eigenvalue transformation (QET) [21,37],

and uniform spectral amplification [37,40]. We demonstrate that the squared norm of the TPQ state, deeply related to the complexity of the quantum simulations, decreases with increasing the number of iterations, but reaches a certain reasonable value if the precise value of the ground-state energy is given. This enables us to explore finite-temperature properties of quantum systems with a quantum computer.

The paper is organized as follows. In Sec. II, we briefly explain the TPQ method. In Sec. III, we explain the quantum techniques used in our scheme. We introduce our TPQ scheme and clarify its complexity in Sec. IV. Some numerical results for the frustrated spin systems are also addressed. A summary is given in the last section.

## II. MICROCANONICAL TPQ STATE

In this section, we briefly explain the microcanonical TPQ state proposed in Ref. [16]. Let  $H$  be the Hamiltonian describing the system of interest with lattice sites  $N$  on a Hilbert space of dimension  $D = 2^N$ , and let  $e_n$  and  $|e_n\rangle$  for  $n = 1, 2, \dots, D$  be the eigenvalues and the corresponding eigenstates, respectively, of the Hamiltonian per site  $h \equiv H/N$  such that  $h|e_n\rangle = e_n|e_n\rangle$ . Without loss of generality, we assume that  $e_{\min} \equiv e_1 \leq e_2 \leq \dots \leq e_D \equiv e_{\max}$ .

In the microcanonical TPQ state method [16], we first prepare a random state  $|\psi_0\rangle$ . While the initial state is a Haar random state in the original definition in Ref. [16], the preparation of the state on a quantum computer would require an exponentially large number of gates as it contains  $D = 2^N$  random variables. Instead, one can employ unitary  $t$ -designs with  $t \geq 2$  that replicates Haar integrals up to the second or higher statistical moment. It is known that a random unitary drawn from the  $n$ -qubit Clifford group yields a unitary 3-design and requires only  $O(N^2/\log N)$  quantum gates [41].

By applying the power of the rescaled Hamiltonian  $(l - h)^k$  with a constant value  $l \geq e_{\max}$  to the initial state, the TPQ state is constructed. The unnormalized  $k$ th TPQ state and corresponding density operator of the microcanonical ensemble are given as [16]

$$|k\rangle \equiv (l - h)^k |\psi_0\rangle, \quad (1)$$

$$\rho_k \equiv \frac{(l - h)^{2k}}{\text{Tr}(l - h)^{2k}}. \quad (2)$$

Namely, the  $k$ th normalized TPQ state  $|\psi_k\rangle \equiv |k\rangle / \| |k\rangle \|$  satisfies, for an arbitrary positive number  $\sigma$ ,

$$\Pr[|\langle \psi_k | A | \psi_k \rangle - \text{Tr} \rho_k A| \geq \sigma] \leq \|A\|^2 \eta_\sigma(N), \quad (3)$$

where  $A$  is an arbitrary observable with polynomially large  $\|A\|^2$  and  $\eta_\sigma(N)$  is a function that vanishes exponentially fast with increasing  $N$ . This inequality means that since the failure probability of the evaluation of the TPQ states exponentially vanishes, only a single realization of the TPQ state is sufficient to evaluate equilibrium values of observables with high probability for large  $N$ . Thus, this method allows one to efficiently obtain the equilibrium values of observables without diagonalization. The proof of the inequality is given in the original paper [16], but is included in Appendix A along with the description of the microcanonical TPQ states for completeness. Equation (3) leads to the fact that  $|\psi_k\rangle$  represents

the equilibrium state specified by the energy density

$$u_k \equiv \langle \psi_k | h | \psi_k \rangle \approx \text{Tr} h \rho_k. \quad (4)$$

One can also obtain genuine thermodynamic variables such as the temperature and entropy of the equilibrium state with the TPQ states. In the TPQ state formalism [16], the inverse temperature  $\beta$  and entropy density  $s$  at the energy density  $u_k$  are calculated by the following formulas:

$$\beta(u_k) = \frac{2k}{N(l - u_k)} + O(N^{-1}), \quad (5)$$

$$s(u_k) = \frac{1}{N} \ln \langle k | k \rangle - \frac{2k}{N} \ln(l - u_k) + \ln 2 + O(N^{-1}). \quad (6)$$

Here, we note that  $k = O(N)$  as  $\beta = O(1)$ .

A key of this method is that one can sequentially calculate thermodynamic quantities of the equilibrium state over a wide range of energies by just applying the power of the rescaled Hamiltonian to the random state. The energy density  $u_k$  decreases gradually down to  $e_{\min}$  as  $k$  increases, i.e.,  $u_0 > u_1 > \dots > e_{\min}$ , and low-temperature properties of the systems can be investigated in accordance with Eq. (5). In addition, the errors of the genuine thermodynamic variables in Eqs. (5) and (6) vanish with increasing  $N$ . Therefore, the TPQ state method may be suitable for quantum computation since it has the potential to treat much larger systems compared with classical computation.

On the other hand, the nonunitary operation is necessary to prepare the TPQ state directly on a quantum computer where operations basically consist of unitary ones. Also, multiple products in Eq. (1) exponentially reduce the success probability in the TPQ state method, which will be discussed later. This means that with the simple TPQ simulation it is hard to study thermodynamic properties at low temperatures.

In the following, combining some techniques proposed recently, we present a method that efficiently implements the TPQ state on a quantum computer to calculate thermodynamic quantities.

## III. MAIN TECHNIQUES

In this section, we introduce three techniques called the block encoding [38,39], QET [21,37], and uniform spectral amplification [37,40] to implement the nonunitary operation, i.e., the power operation  $(l - h)^k$ . Hereafter, the rescaled Hamiltonian  $l - h$  is denoted as  $h'$  for notational simplicity.

### A. Block encoding

Firstly, in order to implement the Hermitian operator  $h'$  ( $\equiv l - h$ ), we employ a block-encoding technique [37–39]. The technique allows us to embed the input  $h'$  on a  $N$ -qubit system register into a larger unitary  $U$  by adding an ancillary  $N_a$ -qubit register. Specifically, for any  $N$ -qubit state  $|\psi\rangle$ , the block-encoding unitary  $W$  is defined such that

$$W |0^{N_a}\rangle \otimes |\psi\rangle = |0^{N_a}\rangle \otimes \frac{h'}{\alpha} |\psi\rangle + |0\psi^\perp\rangle, \quad (7)$$

where  $|0\psi^\perp\rangle$  is an orthogonal state in the ancillary and system qubit register that satisfies  $(\langle 0^{N_a} | \otimes \mathbb{1}^{\otimes N}) |0\psi^\perp\rangle = 0$  with an identity matrix  $\mathbb{1}$  and  $\alpha$  is a constant satisfying

$\alpha \geq \|h'\| (= l - e_{\min})$ . It is also convenient to represent the unitary in matrix form as

$$W = \begin{pmatrix} h'/\alpha & * \\ * & * \end{pmatrix}, \quad (8)$$

where the top-left block denotes the  $|0^{N_a}\rangle \langle 0^{N_a}|$  component.

An example of block encoding is the linear combination of unitaries (LCU) method [38]. The LCU method offers a way to block encode  $h'$  when  $h$  is expressed as a linear combination of unitaries  $\{U_i\}_{i=1}^{N_U}$  such that  $h = \sum_{i=1}^{N_U} \alpha_i U_i$  with coefficients  $\{\alpha_i\}_{i=1}^{N_U}$ . Here, we assume that the coefficients  $\alpha_i$  are positive by incorporating the sign into each unitary  $U_i$ . The block-encoding unitary  $U$  by LCU consists of two unitary operators. The first one is a state preparation unitary operator  $G$  such that

$$G|0^{N_a}\rangle = \frac{\sqrt{l}|0\rangle + \sum_{i=1}^{N_U} \sqrt{\alpha_i}|i\rangle_a}{\sqrt{l + \sum_i \alpha_i}}, \quad (9)$$

where  $\{|i\rangle\}_{i=0}^{N_U}$  are the computational basis. The second one is a controlled unitary operator

$$U = |0\rangle \langle 0| \otimes \mathbb{1} - \sum_{i=1}^{N_U} |i\rangle \langle i| \otimes U_i. \quad (10)$$

One can readily show that  $W = G^\dagger U G$  gives a block encoding of  $h'$ , i.e., satisfies Eq. (7) with  $\alpha = l + \sum_i \alpha_i$ . In this case, the number of the ancillary qubits is  $\lceil \log_2 N_U \rceil$ . According to Ref. [42], the state preparation unitary  $G$  can be implemented with a circuit depth  $\Theta(\log N_U)$  and another  $O(N_U)$  ancillary qubits, and the controlled unitary  $U$  can be realized with a circuit depth  $O[\log(N_U N)]$  and another  $O(N_U N)$  ancillary qubits when each  $U_j$  is a product of single-qubit unitaries such as Pauli operators. Such a set of Hamiltonians covers many kinds of physical models including spin models. In addition, another block-encoding method for general sparse matrices has also been proposed [37,38] that may have advantages depending on the Hamiltonian.

For simplicity, we quantify the complexity of an algorithm with the number of queries of the block-encoding unitary operator  $W$ .

### B. Quantum eigenvalue transformation

The QET [21,37] is a framework for a polynomial transformation of the eigenvalues of a Hermitian matrix encoded in a unitary matrix via QSP [36,38,43]. We define a signal-processing rotation operator via [21]

$$S_\phi \equiv (|0\rangle \langle 0| \otimes \mathbb{1}^{\otimes N_a}) C_{|0^{N_a}\rangle} \text{NOT}(e^{-i\phi\sigma_z} \otimes \mathbb{1}^{\otimes N_a}) \times C_{|0^{N_a}\rangle} \text{NOT}(|0\rangle \langle 0| \otimes \mathbb{1}^{\otimes N_a}) \quad (11)$$

$$\propto e^{i\phi(2|0^{N_a}\rangle \langle 0^{N_a}| - \mathbb{1}^{\otimes N_a})}, \quad (12)$$

where a single ancillary qubit is introduced and  $C_{|0^{N_a}\rangle} \text{NOT}$  is a  $|0^{N_a}\rangle$ -controlled-NOT gate as

$$C_{|0^{N_a}\rangle} \text{NOT} \equiv \sigma^x \otimes |0^{N_a}\rangle \langle 0^{N_a}| + \mathbb{1} \otimes (\mathbb{1}^{\otimes N_a} - |0^{N_a}\rangle \langle 0^{N_a}|). \quad (13)$$

The operator  $S_\phi$  acts as a  $z$  rotation by angle  $\phi$  in the subspace spanned by the basis vectors  $\{|0^{N_a}\rangle \otimes |\psi\rangle, |0^{N_a}\rangle \otimes |\psi^\perp\rangle\}$ . With the block-encoding unitary  $W$  and the rotation operator  $S_\phi$ , QET

is realized, i.e., for any degree- $d$  polynomial  $f(x)$  such that [36,38,43]

- (i)  $f$  has parity- $(d \bmod 2)$ ,
- (ii)  $|f(x)| \leq 1$  for all  $x \in [-1, 1]$ ,
- (iii)  $|f(x)| \geq 1$  for all  $x \in (-\infty, -1] \cup [1, \infty)$ ,
- (iv)  $f(ix)f^*(ix) \geq 1$  for all  $x \in \mathbb{R}$  if  $d$  is even,

there exists a phase sequence  $\Phi = (\phi_1, \phi_2, \dots, \phi_d) \in \mathbb{R}^d$  such that (Theorem 3 in Ref. [21])

$$U_\Phi \equiv \begin{cases} \prod_{j=1}^{d/2} S_{\phi_{2j-1}} W^\dagger S_{\phi_{2j}} W & \text{for even } d \\ S_{\phi_1} W \prod_{j=1}^{(d-1)/2} S_{\phi_{2j}} W^\dagger S_{\phi_{2j+1}} W & \text{for odd } k \end{cases} \quad (14)$$

$$= \begin{pmatrix} f(h'/\alpha) & * \\ * & * \end{pmatrix}, \quad (15)$$

namely,

$$(|0^{N_a}\rangle \otimes \mathbb{1}^{\otimes N}) U_\Phi (|0^{N_a}\rangle \otimes \mathbb{1}^{\otimes N}) = f\left(\frac{h'}{\alpha}\right), \quad (16)$$

where  $f(h'/\alpha) = \sum_{n=1}^D f(\frac{l-e_n}{\alpha}) |e_n\rangle \langle e_n|$  is a polynomial transformation of the eigenvalues of  $h'$ . To implement the power of the Hamiltonian  $h'^k$ , we can directly make use of  $f(x) = x^k$  for odd  $k$  as the degree- $k$  polynomial while for even  $k$ , the function does not satisfy the condition (iv). To implement a real polynomial  $g(x)$  of degree  $k$  satisfying only the conditions (i) and (ii), we can instead add another single qubit and use

$$V_\Phi = |0\rangle \langle 0| \otimes U_\Phi + |1\rangle \langle 1| \otimes U_{-\Phi}, \quad (17)$$

which satisfies

$$g(h'/\alpha) = (|+\rangle \langle +| \otimes |0^{N_a}\rangle \langle 0^{N_a}|) V_\Phi (|+\rangle \langle +| \otimes |0^{N_a}\rangle \langle 0^{N_a}|) = \frac{f(h'/\alpha) + f^*(h'/\alpha)}{2}. \quad (18)$$

The unitary  $V_\Phi$  can be constructed with  $2k$  queries to controlled- $W$  [38]. Also, the corresponding phase sequence  $\Phi$  for a desired function can be efficiently calculated using classical computers.

The QET technique provides a way to efficiently apply polynomial transformations to the Hamiltonian embedded in a block-encoding unitary. However, after applying  $U_\Phi$  ( $V_\Phi$ ) to an input state  $|\psi\rangle$  in the system register, to complete the  $h'^k$  operation, the state must be projected into  $|0^{N_a}\rangle$  in the ancillary qubits, as can be seen from Eq. (16). Hence, if  $|0^{N_a}\rangle$  is observed, the desired state  $\frac{f(h'/\alpha)|\psi\rangle}{\|f(h'/\alpha)|\psi\rangle\|}$  is obtained directly on a quantum computer, and the success probability is given by  $\|f(h'/\alpha)|\psi\rangle\|^2$ . Hence, the probability of obtaining the normalized TPQ state is given by  $\|\langle \psi_0 | (\frac{h'}{\alpha})^{2k} | \psi_0 \rangle\|^2$ , which decays exponentially with increasing  $k$  since  $\|\frac{h'}{\alpha}\| < 1$ . This means that it is computationally hard to study low-temperature properties with just the use of QET. To overcome this problem, we utilize the following technique called uniform spectral amplification [37,40].

### C. Uniform spectral amplification

We employ the uniform spectral amplification technique, which uniformly amplifies the eigenvalues of the embedded Hamiltonian via QET, to avoid the exponential decay of the

success probability. According to Theorem 30 in Ref. [37] (which is a generalization of Theorem 2 in Ref. [40]), for any  $\Lambda \in (\|h'\|, \alpha]$ ,  $\delta \in (0, 1 - \frac{\|h'\|}{\Lambda}]$ , and  $\epsilon \in (0, 1/2)$ , there exists an  $m = O(\frac{\alpha}{\Lambda \delta} \log(\frac{\alpha}{\Lambda \epsilon}))$  and  $\tilde{W} = V_{\Phi}$  operator corresponding to the phase sequence  $\Phi \in \mathbb{R}^m$  such that

$$(|0^{N_a}\rangle \otimes \mathbb{1}^N) \tilde{W} (|0^{N_a}\rangle \otimes \mathbb{1}^N) = \frac{\tilde{h}'}{\Lambda} = \sum_{n=1}^D \frac{l - \tilde{e}_n}{\Lambda} |e_n\rangle \langle e_n|, \quad (19)$$

where the right-hand side is the spectral decomposition of  $\tilde{h}'$  with the eigenvalues  $\{l - \tilde{e}_n\}_{n=1}^D$ , each of which satisfies

$$\frac{|\tilde{e}_n - e_n|}{\Lambda} < \epsilon. \quad (20)$$

As the above statement is slightly different from the original theorem only in terms of the notation, a brief derivation of it is provided in Appendix B. Constructing  $\tilde{W}$  requires  $O(\frac{\alpha}{\Lambda \delta} \log(\frac{\alpha}{\Lambda \epsilon}))$  queries to controlled- $W$ . This technique is derived from an approximate polynomial of the truncated linear function  $\frac{\alpha}{\Lambda}x$  through the error function [37,40]. Because of the uniform spectral amplification, the normalization factor  $\alpha$  of the encoded Hamiltonian can be reduced to  $\Lambda$  with exponentially small error  $\epsilon$  with respect to the complexity. However, it requires knowledge of the upper bound  $\Lambda$  of  $\|h'\| = l - e_{\min}$ , i.e., the lower bound of the minimum eigenvalue of  $h$ .

#### IV. QUANTUM ALGORITHM AND THE COMPLEXITY

Our algorithm is straightforwardly constructed by combining the three techniques introduced in Sec. III hierarchically. We realize the operation  $\tilde{h}'^k$  through the QET of a polynomial  $x^k$  using the amplified block-encoding unitary  $\tilde{W}$ , which is constructed from  $W$ . For odd  $k$ , we can implement  $V = U_{\Phi}$  such that

$$(|0^{N_a}\rangle \otimes \mathbb{1}^N) V (|0^{N_a}\rangle \otimes \mathbb{1}^N) = \left(\frac{\tilde{h}'}{\Lambda}\right)^k. \quad (21)$$

For even  $k$ , we have to instead use  $V_{\Phi}$  with controlled- $\tilde{W}$ . After the operation, if  $|0^{N_a}\rangle$  is observed in the ancillary qubits, we obtain the normalized approximated  $k$ th TPQ state

$$|\tilde{\psi}_k\rangle \equiv \frac{\tilde{h}'^k |\psi_0\rangle}{\|\tilde{h}'^k |\psi_0\rangle\|}, \quad (22)$$

which somewhat differs only in the eigenvalues of the Hamiltonian, and the probability of success, i.e., the probability of observing  $|0^{N_a}\rangle$  is

$$\frac{\langle \psi_0 | \tilde{h}'^{2k} | \psi_0 \rangle}{\Lambda^{2k}}, \quad (23)$$

which depends on the initial random state. Averaging over the random state we roughly evaluate the probability for sufficiently large  $k$  required for the calculation of thermodynamic quantities at low temperatures as

$$O\left[\frac{1}{D} \sum_{n=1}^D \left(\frac{l - \tilde{e}_n}{\Lambda}\right)^{2k}\right] = O\left[\frac{1}{D} \left(\frac{l - e_{\min}}{\Lambda}\right)^{2k}\right], \quad (24)$$

where we have assumed that  $\epsilon \ll 1/k$  to neglect the small error.

Since the probability given in Eq. (24) is still tiny in any case as the denominator is the dimension of the system, we also use the amplitude amplification technique [37,44] to complete the implementation of  $\tilde{h}'^k$ . The technique allows for amplifying the success probability to a constant  $O(1)$ . In this case,

$$O\left[\sqrt{D} \left(\frac{\Lambda}{l - e_{\min}}\right)^k\right], \quad (25)$$

iterations of amplitude amplification are required, and this can be implemented via an additional layer of QSP [37].

Thus, our algorithm provides an efficient way to multiply a random state by  $h^k$  and obtain the approximate normalized TPQ state on a quantum computer with constant probability. Specifically, we can implement a quantum algorithm  $\tilde{V}$  that satisfies

$$\frac{(|0^{N_a}\rangle \otimes \mathbb{1}^N) \tilde{V} (|0^{N_a}\rangle \otimes |\psi_0\rangle)}{\|(|0^{N_a}\rangle \otimes \mathbb{1}^N) \tilde{V} (|0^{N_a}\rangle \otimes |\psi_0\rangle)\|} = |\tilde{\psi}_k\rangle \quad (26)$$

and is constructed by three layers of QSP: the amplitude amplification, QET, and uniform spectral amplification. The approximate TPQ state  $|\tilde{\psi}_k\rangle$  represents an ensemble of the density matrix  $\tilde{\rho}_k \equiv \frac{\tilde{h}'^{2k}}{\text{Tr} \tilde{h}'^{2k}}$  by which  $\rho_k$  is approximated, and it is noted that the difference between  $|\tilde{\psi}_k\rangle$  and  $\tilde{\rho}_k$  is exponentially small from Eq. (3). Thus, the error in the approximate TPQ state is evaluated by the error between the corresponding density matrices: for  $\epsilon' \in (0, 1)$

$$\frac{1}{2} \|\tilde{\rho}_k - \rho_k\|_1 < \epsilon', \quad (27)$$

where  $\|\cdot\|_1$  denotes the trace norm. From the relation between  $\epsilon$  and  $\epsilon'$  discussed in Appendix C, one can get the TPQ state with the desired precision as in Eq. (27) if the error  $\epsilon$  satisfies

$$\epsilon < \frac{l - e_{\max}}{2k\Lambda} \epsilon' (1 - \epsilon'). \quad (28)$$

Therefore, we can conclude our algorithm in terms of the query complexity of the block-encoding unitary  $W$  as

$$O\left[\left(\frac{\Lambda}{l - e_{\min}}\right)^k \sqrt{D} k \frac{\alpha}{\Lambda \delta} \log\left(\frac{2k\alpha}{l - e_{\max}} \frac{1}{\epsilon'}\right)\right], \quad (29)$$

where each term represents the contributions from the amplitude amplification, QET of  $x^k$ , and uniform spectral amplification, respectively in that order.

In addition, if the ground-state energy is given with some precision, we can set  $\Lambda = l - e_{\min}(1 \pm \delta')$  where  $\delta' > 0$  is a precision parameter, and the sign is taken so that  $\Lambda > l - e_{\min}$ . When  $\delta'$  is chosen to be small as  $\delta' \ll 1/k$ , the exponential increase with respect to  $k$  can be neglected and the complexity is then given as

$$O\left[\sqrt{D} k \frac{\alpha}{\Lambda \delta} \log\left(\frac{2k\alpha}{l - e_{\max}} \frac{1}{\epsilon'}\right)\right]. \quad (30)$$

This means that the precision of the ground-state energy of the Hamiltonian plays a crucial role and the exponential increase of the complexity can be suppressed in the case with  $\delta' = O(1/k)$ . We note that if the ground-state energy is not

given with such precision, the overall complexity grows exponentially with  $k$  in our method, making it almost impossible to construct the low-temperature TPQ states. The problem of estimating ground-state energies of local Hamiltonians is QMA (Quantum Merlin Arthur) complete, which means that obtaining the ground-state energies cannot be done efficiently even on a quantum computer. However, quantum algorithms using the variational method [45], adiabatic evolution [46], the filtering method [47,48], and Lanczos methods [49–52] have been proposed that can efficiently find the ground-state energy with some additional assumptions. Therefore, by using the value obtained with the algorithms, the exponential decay of the probability with respect to  $k$  can be suppressed, and exploring low-temperature properties might be performed efficiently on a quantum computer.

More specifically, we consider the  $S = 1/2$  quantum spin systems, where the Hamiltonian is, in general, represented by a linear combination of tensor products of Pauli operators. Then, the block-encoding unitary  $W$  is implemented by means of the LCU method with  $\alpha = O(1)$ ,  $N_U = O(N)$ . Noting that  $\delta < |\delta'| = O(1/k)$  and  $\Lambda = O(1)$ , the gate complexity is given as

$$O\left[Nk^2\sqrt{D}\log\left(\frac{k}{\epsilon'}\right)\right]. \quad (31)$$

Since the computational complexity for one iteration of the TPQ method on a classical computer constructed by vector and (sparse) matrix operation is  $O(ND)$ , a quadratic speedup should be realized more or less except for the logarithmic factors. Therefore, our scheme has a potential method to investigate low-temperature properties of quantum systems in large systems.

Now, we calculate the squared norm  $\frac{\langle k|k\rangle}{\Lambda^{2k}}$  using the classical TPQ state method to simply confirm that the success probability is  $O(D^{-1})$  if  $\delta'$  is chosen to be  $O(1/k)$  by using the uniform spectral amplification. To this end, we consider the Heisenberg model on a kagome lattice (KH model) and Kitaev models with a coupling constant  $J$ , as examples of frustrated quantum spin systems. In these cases, the corresponding Hamiltonians can be easily encoded into unitary by the LCU method with  $\alpha = l + 6J$  and  $\alpha = l + 3J/2$ , respectively. The details of these models will be explained in Appendix D. Here, the TPQ state simulations are performed from 25 independent Haar random states of  $|\psi_0\rangle$  on a classical computer, by setting the parameter  $l = e_{\max} + 0.001$ . Figure 1 shows the squared norm  $\langle k|k\rangle/\Lambda^{2k}$  for both models with  $N = 30$ . When the bare TPQ state method is applied without the uniform spectral amplification technique, the squared norm rapidly decreases since  $l - e_{\min} < \alpha$ , which is clearly shown as the dotted line in Fig. 1. On the other hand, we find that the squared norm decreases slowly with small  $\delta'$ , and is  $O(D^{-1})$  in a region  $k \in [0, O(1/\delta')]$  for any  $\delta'$ . This suggests that the knowledge of the ground-state energy  $e_{\min}$  with a precision of  $O(1/k)$  suppresses the exponential decay in the success probability or the exponential increase in complexity. The inset of Fig. 1 shows the temperature as a function of  $k$  in the TPQ state simulations. It is found that the increase of  $k$  monotonically decreases the temperature. In general, there exists the characteristic temperature  $T^*$  that depends on the model. Namely,  $T^* \sim 0.2J$  for the KH model

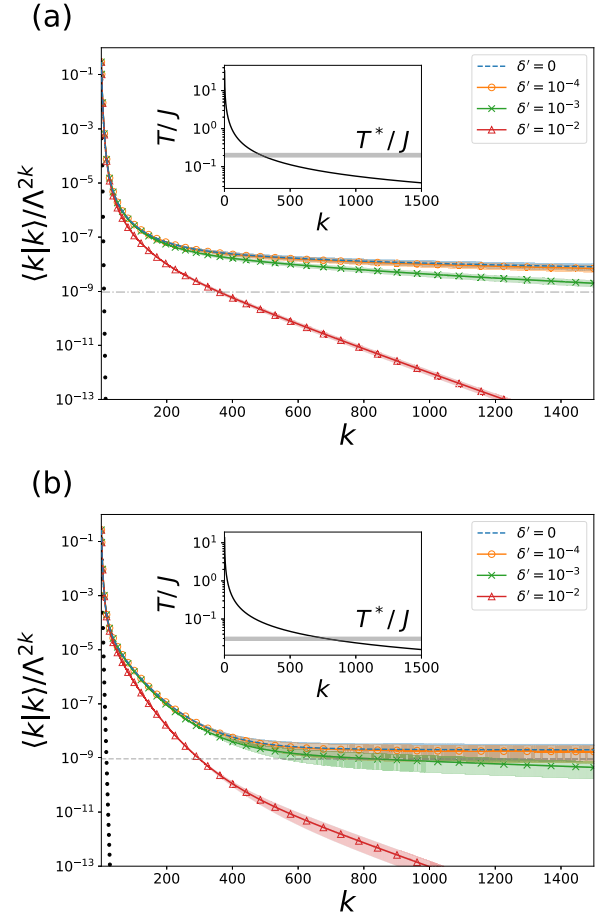


FIG. 1. The squared norm  $\langle k|k\rangle/\Lambda^{2k}$  as a function of  $k$  in the (a) KH and (b) Kitaev models with  $N = 30$  when  $\delta' = 0, 10^{-4}, 10^{-3}$ , and  $10^{-2}$ . The shaded areas stand for the standard deviation of the results. The TPQ results without the uniform spectral amplification are represented by the dotted line. The gray dashed line represents  $D^{-1} = 2^{-30}$ .

and  $T^* \sim 0.03J$  for the Kitaev model (see Appendix D). It is found that  $k \sim 1500$  ( $50N$ ) iterations are enough to reach the characteristic temperature. These results imply that thermodynamic properties can be explored within a reasonable computational cost if the ground-state energy is obtained with an accuracy of  $O[(50N)^{-1}]$ . It is expected that our quantum scheme is applied to interesting quantum systems and their low-temperature properties would be clarified.

## V. SUMMARY

We have presented the quantum algorithm for the TPQ state method, combining the block-encoding, uniform spectral amplification, QET, and amplitude amplification techniques. If the precise value of the ground-state energy is given, the computational cost in the power operation of the rescaled Hamiltonian constructing the TPQ states is exponentially reduced. This would enable us a quadratic speedup except for the polylogarithmic factors compared with the classical simulation. Therefore, our work should stimulate further theoretical studies in condensed matter physics with quantum computers.

### ACKNOWLEDGMENTS

We would like to thank K. Fujii for his valuable discussions. This work was supported by Grant-in-Aid for Scientific Research from JSPS, KAKENHI Grants No. JP22K03525, No. JP21H01025, and No. JP19H05821 (A.K.).

### APPENDIX A: REVIEW OF MICROCANONICAL TPQ STATE

In this Appendix, we review the microcanonical thermal pure quantum state introduced by Sugiura and Shimizu in Ref. [16]. Specifically, we derive the evaluations of genuine thermodynamic variables such as the temperature and entropy density in Eqs. (5) and (6) and show that the states are thermal pure quantum states, i.e., satisfy Eq. (3).

Firstly, we derive the energy density distribution of the smooth microcanonical ensemble  $\rho_k = \frac{(l-h)^{2k}}{\text{Tr}(l-h)^{2k}}$  corresponding to the TPQ state. Denoting the density of microstates  $g(u)$  as a function of energy density  $u$ , we obtain the entropy density as

$$s(u) = \frac{1}{N} \ln g(u). \quad (\text{A1})$$

Then, the energy density distribution of the density matrix  $\rho_k$  can be written as [16,53]

$$r_k(u) \equiv g_N(u)(l-u)^{2k} = \exp[N\xi_k(u)], \quad (\text{A2})$$

where  $\xi_k(u) \equiv \frac{2k \ln(l-u)}{N} - s(u)$ . This energy density distribution takes the maximum at  $u = u_k^*$  that satisfies  $\frac{\partial}{\partial u} \xi_k(u) = 0$ , i.e.,

$$\beta(u_k^*) \equiv \left. \frac{\partial}{\partial u} s(u) \right|_{u=u_k^*} = \frac{2k}{N(l-u_k^*)}. \quad (\text{A3})$$

Expanding  $\xi_k(u)$  around  $u_k^*$  and noting  $\frac{\partial^2}{\partial u^2} \xi_k(u)|_{u=u_k^*} < 0$  since  $\frac{\partial}{\partial u} \beta(u)|_{u=u_k^*} \leq 0$ , we get

$$\xi_k(u) = \xi_k(u_k^*) - \frac{1}{2} |\xi_k''(u_k^*)| (u - u_k^*)^2 + \dots, \quad (\text{A4})$$

where  $\xi_k''(u_k^*) \equiv \frac{\partial^2}{\partial u^2} \xi_k(u)|_{u=u_k^*}$ . Thus, the energy density distribution  $r_k$  behaves like a Gaussian distribution with the peak at  $u_k^*$  and the small variance  $\frac{1}{N|\xi_k''(u_k^*)|}$ . Therefore,  $\rho_k$  represents the equilibrium state with the energy specified by  $u = u_k^*$ .

We can obtain thermodynamic variables such as the entropy and temperature with the ensemble. Using Eq. (A4) and applying Laplace's method [53], we have

$$\text{Tr}(l-h)^{2k} = \int_{-\infty}^{\infty} du \exp[N\xi_k(u)] \quad (\text{A5})$$

$$= \exp \left[ -N \left( \frac{4k}{N} \ln \frac{l-u_{2k}^*}{l-u_k^*} + 2s(u_k^*) - s(u_{2k}^*) \right) + O(\log N) \right]. \quad (\text{A6})$$

Then the energy density is also obtained as

$$u_{\rho_k} \equiv \text{Tr} h \rho_k = \frac{\int_{-\infty}^{\infty} du u \exp[N\xi_k(u)]}{\int_{-\infty}^{\infty} du \exp[N\xi_k(u)]} \quad (\text{A7})$$

$$= u_k^* + O(N^{-1}). \quad (\text{A8})$$

Hence, using Eqs. (A3) and (A6), we obtain the thermodynamic variables at the specified energy  $u_k^*$  with the smooth microcanonical ensemble as

$$s(u_k^*) = \frac{1}{N} \ln \text{Tr}(l-h)^{2k} - \frac{2k}{N} \ln(l-u_k^*) + O(N^{-1} \log N), \quad (\text{A9})$$

$$\beta(u_k^*) = \frac{2k}{N(l-u_k^*)} + O(N^{-1}). \quad (\text{A10})$$

Here, we note that  $u_k$  and  $\text{Tr}(l-h)^{2k}$  can be calculated through the TPQ states, as discussed below.

We show that the  $k$ th TPQ state

$$|\psi_k\rangle = \frac{(l-h)^k |\psi_0\rangle}{\|(l-h)^k |\psi_0\rangle\|} \quad (\text{A11})$$

is a thermal pure quantum state for the smooth microcanonical ensemble  $\rho_k$ , namely, satisfies Eq. (3) in the main text. Firstly, we assume that the initial random state  $|\psi_0\rangle$  is generated by at least unitary 2-design and written as

$$|\psi_0\rangle = \sum_{i=1}^D c_i |i\rangle, \quad (\text{A12})$$

where  $\{|i\rangle\}_{i=1,\dots,D}$  denote arbitrary orthonormal basis states of the  $D$ -dimensional Hilbert space and  $c_i$  are random variables that satisfy  $\sum_i |c_i|^2 = 1$  following the unitary design. Then, using the Haar integrals up to the second moment, we get [54]

$$E[|c_i|^2] = \frac{1}{D}, \quad (\text{A13})$$

$$E[|c_i|^2 |c_j|^2] = \frac{1}{D(D+1)} \quad \text{for } i \neq j, \quad (\text{A14})$$

$$E[|c_i|^4] = \frac{2}{D(D+1)}, \quad (\text{A15})$$

where  $E[\cdot]$  denotes the expectation values over the random variables  $\{c_i\}_i$  and all combinations other than the above such as  $c_i c_j$  are zero below the fourth order. Using Eqs. (A13), (A14), and (A15), the expectation value and relative variance of the normalization factor  $\langle k|k \rangle$  can be calculated as

$$E[\langle k|k \rangle] = \frac{\text{Tr}(l-h)^{2k}}{D}, \quad (\text{A16})$$

$$\text{Var} \left[ \frac{\langle k|k \rangle}{E[\langle k|k \rangle]} \right] = \frac{D}{1+D} \frac{\text{Tr}(l-h)^{4k}}{[\text{Tr}(l-h)^{2k}]^2} - \frac{1}{D+1} \quad (\text{A17})$$

$$\leq \text{Tr} \rho_k^2 \quad (\text{A18})$$

$$= \exp \left[ N \left( \frac{2k}{N} \ln(l-u_k^*) - s(u_k^*) \right) + O(\log N) \right], \quad (\text{A19})$$

where we have used Eq. (A6). Here, we find that  $\frac{4k}{N} \ln \frac{l-u_{2k}^*}{l-u_k^*} + 2s(u_k^*) - s(u_{2k}^*) > 0$  for all  $k$  by using the fact that  $u_k^* > u_{2k}^*$  and  $\frac{\partial s(u)}{\partial u} > 0$ , and then the purity of the density matrix  $\text{Tr} \rho_k^2$  exponentially decays with increasing the system size  $N$ . Thus, this variance is exponentially small in the system size  $N$ .

Next, we will use  $f \equiv \langle k|A|k \rangle$  and  $g \equiv \langle k|k \rangle$  to simplify the notations. Then,  $\frac{f}{g} = \langle \psi_k|A|\psi_k \rangle$  and  $\frac{E[f]}{E[g]} = \text{Tr} A \rho_k$  denote the evaluations of the observable  $A$  in the TPQ state  $|\psi_k\rangle$

and the density matrix  $\rho_k$ , respectively. Hence, we provide proof that the TPQ states satisfy Eq. (3) by making use of Markov's inequality

$$\Pr \left[ \left| \frac{f}{g} - \frac{E[f]}{E[g]} \right| > \sigma \right] > \frac{1}{\sigma^2} E \left[ \left| \frac{f}{g} - \frac{E[f]}{E[g]} \right|^2 \right], \quad (\text{A20})$$

and showing that the error between  $\frac{f}{g}$  and  $\frac{E[f]}{E[g]}$  is exponentially small. As the relative variance of  $g$  is small, we use a multivariate Taylor expansion up to first order in  $\text{Var}[\frac{g}{E[g]}]$  as [18]

$$E \left[ \frac{f}{g} \right] \approx \frac{E[f]}{E[g]} - \frac{\text{Cov}[f, g]}{E[g]^2} + \frac{E[f]}{E[g]} \text{Var} \left[ \frac{g}{E[g]} \right], \quad (\text{A21})$$

where  $\text{Cov}[f, g]$  is the covariance defined by  $\text{Cov}[f, g] = E[f g] - E[f]E[g]$ . Calculating each term in the expansion with Eqs. (A13), (A14), and (A15), we obtain

$$E \left[ \frac{f}{g} \right] \approx \text{Tr} A \rho_k + \frac{D}{D+1} \text{Tr} \rho_k^2 (\text{Tr} A \rho_k - \text{Tr} A \rho_{2k}). \quad (\text{A22})$$

Similarly, we evaluate the expectation value of  $(\frac{f}{g})^2$  using a multivariate Taylor expansion as

$$E \left[ \left( \frac{f}{g} \right)^2 \right] \approx \frac{E[f]^2}{E[g]^2} + \frac{\text{Var}[f]}{E[g]^2} - 4 \frac{E[f]}{E[g]^3} \text{Cov}[f, g] + 3 \frac{E[f]^2}{E[g]} \text{Var} \left[ \frac{g}{E[g]} \right]. \quad (\text{A23})$$

Using Eqs. (A21) and (A23), we have

$$E \left[ \left| \frac{f}{g} - \frac{E[f]}{E[g]} \right|^2 \right] \approx \frac{\text{Var}[f]}{E[g]^2} - 2 \frac{E[f]}{E[g]^3} \text{Cov}[f, g] + \frac{E[f]^2}{E[g]^2} \text{Var} \left[ \frac{g}{E[g]} \right] \quad (\text{A24})$$

$$= \frac{D}{D+1} \text{Tr} \rho_k^2 \left\{ (\text{Tr} A \rho_k)^2 - 2 \text{Tr} A \rho_k \text{Tr} A \rho_{2k} + \frac{\text{Tr} [(l-h)^{2k} A]^2}{\text{Tr} (l-h)^{4k}} \right\} \quad (\text{A25})$$

$$\leq \text{Tr} \rho_k^2 4 \|A\|^2, \quad (\text{A26})$$

where we have used the fact that

$$\frac{\text{Tr} [(l-h)^{2k} A]^2}{\text{Tr} (l-h)^{4k}} \leq \sum_{e_i, e_j} \frac{(l-e_i)^{4k} + (l-e_j)^{4k}}{2 \text{Tr} (l-h)^{4k}} | \langle e_i | A | e_j \rangle |^2 \quad (\text{A27})$$

$$\leq \|A\|^2. \quad (\text{A28})$$

Therefore, we obtain

$$\Pr [ | \langle \psi_k | A | \psi_k \rangle - \text{Tr} A \rho_k | \geq \sigma ] \leq \|A\|^2 \frac{4 \text{Tr} \rho_k^2}{\sigma^2}, \quad (\text{A29})$$

and this inequality shows that the failure probability of the TPQ states exponentially vanishes from Eq. (A6) as indicated in Eq. (3). Note that the above property is derived by only using Eqs. (A13), (A14), and (A15), i.e., the Haar integrals up to the second moment. Therefore, it would be sufficient to use unitary  $t$ -designs with  $t \geq 2$  for generating the initial random state.

## APPENDIX B: NOTATIONAL CHANGES FROM THE ORIGINAL THEOREM OF THE UNIFORM SPECTRAL AMPLIFICATION TECHNIQUE

In this section, we shortly derive the notational change from the original theorem in the uniform spectral amplification technique introduced in the main text. Theorem 30 in Ref. [37] states as follows.

Let  $\gamma > 1$  and let  $\delta, \epsilon \in (0, \frac{1}{2})$ . Suppose that  $\langle 0^{N_a} | U | 0^{N_a} \rangle = \sum_i \lambda_i | \lambda_i \rangle \langle \lambda_i |$  is an eigenvalue decomposition, and  $\max_i \{ |\lambda_i| \} \leq \frac{1-\delta}{\gamma}$ . Then there is an  $m = O(\frac{\gamma}{\delta} \log(\frac{\gamma}{\epsilon}))$  and an efficiently computable  $\Phi \in \mathbb{R}^m$  such that

$$\begin{aligned} & ( \langle + | \otimes \langle 0^{N_a} | \otimes \mathbb{1}^{\otimes N} ) V_{\Phi} ( | + \rangle \otimes | 0^{N_a} \rangle \otimes \mathbb{1}^{\otimes N} ) \\ & = \sum_i \tilde{\lambda}_i | \lambda_i \rangle \langle \lambda_i |, \end{aligned} \quad (\text{B1})$$

where each eigenvalue  $\tilde{\lambda}_i$  satisfies

$$\left\| \frac{\tilde{\lambda}_i}{\gamma \lambda_i} - 1 \right\| < \epsilon. \quad (\text{B2})$$

Here it is noted that the original theorem uses singular values  $\varsigma_i$  for a general matrix instead of eigenvalues  $\lambda_i$ .

In the main text, the eigenvalues are replaced as  $\lambda_i = \frac{l-e_i}{\alpha}$  and  $\tilde{\lambda}_i = \frac{l-\tilde{e}_i}{\Lambda}$ , and then we used the notations as  $\gamma = \alpha/\Lambda$ ,  $\Lambda \geq \frac{l-e_{\min}}{1-\delta}$ ,  $\frac{\|e_i - \tilde{e}_i\|}{\Lambda} < \epsilon$ , and  $m = O(\frac{\alpha}{\Lambda} \frac{1}{\delta} \log(\frac{\alpha}{\Lambda} \frac{1}{\epsilon}))$ .

## APPENDIX C: RELATION BETWEEN $\epsilon$ AND $\epsilon'$

In this section, we derive Eq. (28) in the main text, which is a relationship between the approximation error  $\epsilon'$  given in Eq. (20) and the error  $\epsilon$  given in Eq. (27). Firstly, noting that the density matrices  $\rho_k$  and  $\tilde{\rho}_k$  have the common eigenstates  $\{ |e_i\rangle \}_i$ , we obtain the upper bound of the trace distance as

$$\frac{1}{2} \| \rho_k - \tilde{\rho}_k \|_1 = \frac{1}{2} \sum_i \left| \frac{(l-e_i)^{2k}}{\text{Tr} (l-h)^{2k}} - \frac{(l-\tilde{e}_i)^{2k}}{\text{Tr} (l-\tilde{h})^{2k}} \right| \quad (\text{C1})$$

$$\leq \frac{1}{2} \sum_{i,j} \frac{|(l-e_i)^{2k} (l-\tilde{e}_j)^{2k} - (l-\tilde{e}_i)^{2k} (l-e_j)^{2k}|}{\text{Tr} (l-h)^{2k} \text{Tr} (l-\tilde{h})^{2k}} \quad (\text{C2})$$

$$= \frac{1}{2} \sum_{i,j} \frac{(l-e_i)^{2k} (l-\tilde{e}_j)^{2k} \left| 1 - \left( \frac{l-\tilde{e}_i}{l-e_i} \frac{l-e_j}{l-\tilde{e}_j} \right)^{2k} \right|}{\text{Tr} (l-h)^{2k} \text{Tr} (l-\tilde{h})^{2k}}. \quad (\text{C3})$$

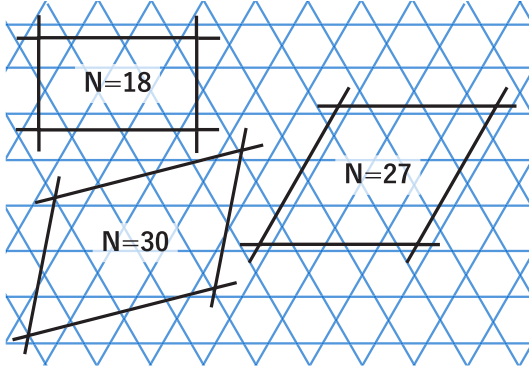


FIG. 2. Finite-size clusters of the kagome lattice used in the TPQ simulations. The boundaries exhibit periodic boundary conditions.

Here, using the Eq. (20), we get

$$\frac{1 - \kappa\epsilon}{1 + \kappa\epsilon} < \frac{l - \tilde{e}_i l - e_j}{l - e_i l - \tilde{e}_j} < \frac{1 + \kappa\epsilon}{1 - \kappa\epsilon}, \quad (\text{C4})$$

where  $\kappa \equiv \frac{\Lambda}{l - e_{\max}}$  when  $\epsilon < \kappa^{-1}$ . Hence, we can evaluate the absolute value in the numerator factor in Eq. (C3) as

$$\left| 1 - \left( \frac{l - \tilde{e}_i l - e_j}{l - e_i l - \tilde{e}_j} \right)^{2k} \right| < \left( \frac{1 + \kappa\epsilon}{1 - \kappa\epsilon} \right)^{2k} - 1. \quad (\text{C5})$$

Therefore, we get the upper bound of the trace distance as

$$\frac{1}{2} \|\rho_k - \tilde{\rho}_k\|_1 \leq \frac{1}{2} \left\{ \left( \frac{1 + \kappa\epsilon}{1 - \kappa\epsilon} \right)^{2k} - 1 \right\}. \quad (\text{C6})$$

Then, assuming the right-hand side is less than  $\epsilon'$  and solving the inequality for  $\epsilon$ , we finally show that

$$\epsilon < \frac{1}{\kappa} \frac{\epsilon'}{2k} (1 - \epsilon') < \frac{1}{\kappa} \left\{ 1 - \frac{2}{1 + (1 + 2\epsilon')^{1/2k}} \right\}, \quad (\text{C7})$$

where we have used the fact that  $\frac{x(1-x)}{2k} < 1 - \frac{2}{1+(1+2x)^{1/2k}}$  for  $x \in (0, 1)$  and  $k \geq 1$ .

#### APPENDIX D: DETAILS OF THE FRUSTRATED QUANTUM SPIN MODELS

Here, we explain the details of the models used in the TPQ simulations. In frustrated spin systems, low-energy states should play an important role and the characteristic temperatures are relatively low, compared to unfrustrated systems. In fact, low-temperature peak or shoulder in specific heat has been discussed in some systems. Now, we treat the KH and Kitaev models as examples of the frustrated models. To make our discussions clear, we set  $l = e_{\max} + 0.001$ .

##### 1. The Heisenberg model on the kagome lattice

First, we consider the Heisenberg model on the kagome lattice (KH model) with antiferromagnetic couplings as one of the systems with geometrical frustration, which is schematically shown in Fig. 2. The system includes triangle structures and each site connects the four nearest-neighbor sites. The

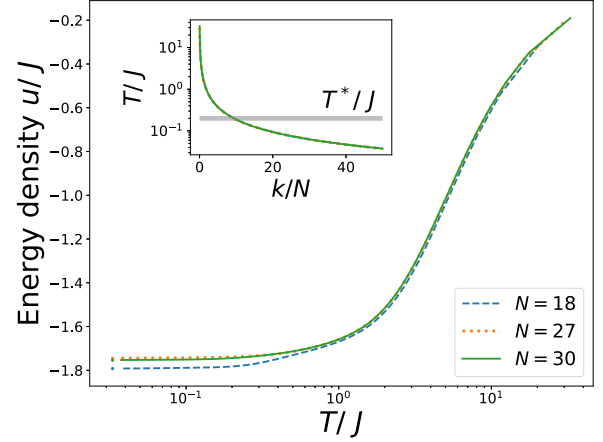


FIG. 3. Internal energy in the Heisenberg model on the kagome lattice with  $N = 18, 27$ , and  $30$ . The inset shows the temperature as a function of  $k$ . The error bars stand for the standard deviation of the results. Circles represent the ground-state energies for the corresponding system.

model Hamiltonian is given as

$$H = J \sum_{\langle ij \rangle} \sigma_i \cdot \sigma_j, \quad (\text{D1})$$

where  $\sigma_i = (\sigma_i^x, \sigma_i^y, \sigma_i^z)$ ,  $\sigma_i^\mu$  is the  $\mu$  component of the Pauli matrix at the  $i$ th site, and the index  $\langle ij \rangle$  represents the summation over the connecting spin pairs.  $J (> 0)$  is the antiferromagnetic exchange coupling.

For the clusters with  $N = 18$  and  $27$ , we evaluate temperatures and internal energies by means of 100 independent TPQ states. By contrast, the numerical cost is high for the cluster with  $N = 30$ , and 25 independent states are treated. The internal energy is shown in Fig. 3. At low temperatures, the internal energy strongly depends on the size and/or shape of the system. This means that low-energy states play an important role in the kagome-Heisenberg model. It has been clarified that there exists shoulder behavior in the specific heat and its characteristic temperature is deduced as  $T^* \sim 0.3J$  [17]. The inset of Fig. 3 shows the temperature as a function of the scaled iteration  $k/N$ . We find that the curves little depend on  $k/N$ . Therefore, the TPQ state at  $T = T^*$  is obtained with  $k \sim 10N$  when the parameters are appropriately given.

##### 2. The Kitaev model on a honeycomb lattice

We consider the Kitaev model on a honeycomb lattice [55], which is composed of direction-dependent Ising-like interactions and is known to be the exactly solvable system with bond frustration. The Hamiltonian is given by

$$H = -J \sum_{\langle i,j \rangle_x} \sigma_i^x \sigma_j^x - J \sum_{\langle i,j \rangle_y} \sigma_i^y \sigma_j^y - J \sum_{\langle i,j \rangle_z} \sigma_i^z \sigma_j^z, \quad (\text{D2})$$

where  $\langle i, j \rangle_\mu$  represents the nearest-neighbor pair on the  $\mu (= x, y, z)$  bonds. The  $x$ ,  $y$ , and  $z$  bonds are shown as red, blue, and green lines in Fig. 4(a).

$J$  is the exchange coupling between the nearest-neighbor spins. In the Kitaev model, there exists a local conserved quantity defined at each plaquette  $p$  composed of the sites



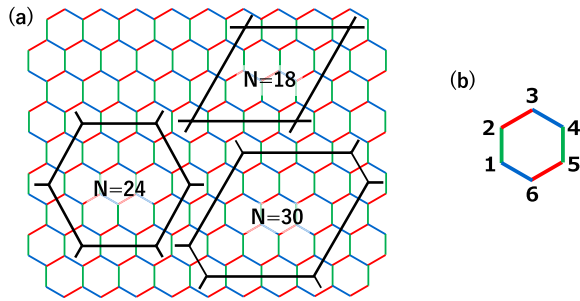


FIG. 4. (a) Finite-size clusters of the Kitaev model on the honeycomb lattice used in the TPQ simulations. The boundaries exhibit periodic boundary conditions. Red, blue, and green lines represent  $x$ ,  $y$ , and  $z$  bonds, respectively. (b) Plaquette with sites marked 1–6 is shown for the corresponding operator  $W_p$  (see text).

labeled as  $1, 2, \dots, 6$  [see Fig. 4(b)],  $W_p = \sigma_1^x \sigma_2^y \sigma_3^z \sigma_4^x \sigma_5^y \sigma_6^z$ . It is known that due to the existence of the local conserved quantities, the ground state is the quantum spin liquid, where the spin degrees of freedom are fractionalized into itinerant Majorana fermions and fluxes. This leads to two distinct characteristic energy scales. In fact, we find in Fig. 5 two shoulder structures appear in the internal energy around  $T \sim 0.1J$  and  $\sim 0.8J$ . This behavior is clearly found as a double-peak structure in the specific heat [2], and these peaks are located at  $T^* \sim 0.03J$  and  $T^{**} \sim 1.5J$ . The characteristic temperature  $T^*$  is relatively low due to this fractionalization phenomenon.

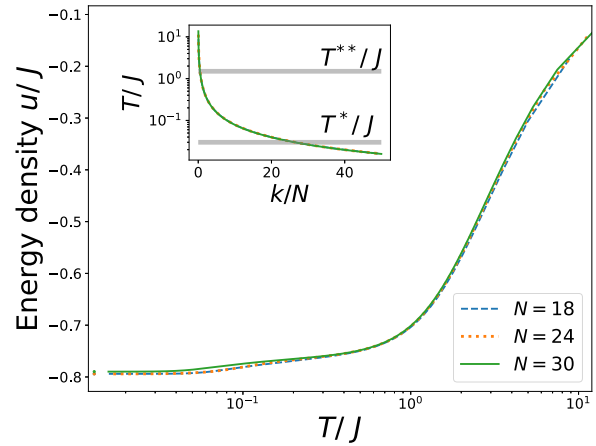


FIG. 5. Internal energy in the Kitaev model with  $N = 18, 24$ , and  $30$ . The inset shows the temperature as a function of  $k$ . The results are obtained from the TPQ state generated from 100 and 25 samples of the initial random state for  $N = 18, 27$ , and  $N = 30$ , respectively, and the error bars stand for the standard deviation of the results. Circles represent the ground-state energies for the corresponding system.

The inset of Fig. 5 shows that the temperature is a function of  $k/N$ . We find that the curve of the temperatures is well scaled by  $k/N$ , which is similar to that of the KH model. Therefore, the TPQ state at the lower characteristic temperature  $T = T^*$  is obtained with  $k \sim 30N$  when appropriate parameters are given.

[1] T. Nakamura, *Phys. Rev. B* **57**, R3197(R) (1998).  
 [2] J. Nasu, M. Udagawa, and Y. Motome, *Phys. Rev. B* **92**, 115122 (2015).  
 [3] R. P. Feynman, *Feynman and Computation* (CRC Press, Boca Raton, 2018), pp. 133–153.  
 [4] A. Riera, C. Gogolin, and J. Eisert, *Phys. Rev. Lett.* **108**, 080402 (2012).  
 [5] A. N. Chowdhury and R. D. Somma, *Quantum Inf. Comput.* **17**, 41 (2017).  
 [6] D. Poulin and P. Wocjan, *Phys. Rev. Lett.* **103**, 220502 (2009).  
 [7] E. Bilgin and S. Boixo, *Phys. Rev. Lett.* **105**, 170405 (2010).  
 [8] J. Wu and T. H. Hsieh, *Phys. Rev. Lett.* **123**, 220502 (2019).  
 [9] D. Zhu, S. Johri, N. M. Linke, K. Landsman, C. Huerta Alderete, N. H. Nguyen, A. Matsuura, T. Hsieh, and C. Monroe, *Proc. Natl. Acad. Sci. USA* **117**, 25402 (2020).  
 [10] A. N. Chowdhury, G. H. Low, and N. Wiebe, [arXiv:2002.00055](https://arxiv.org/abs/2002.00055).  
 [11] S. Lu, M. C. Bañuls, and J. I. Cirac, *PRX Quantum* **2**, 020321 (2021).  
 [12] K. Temme, T. J. Osborne, K. G. Vollbrecht, D. Poulin, and F. Verstraete, *Nature (London)* **471**, 87 (2011).  
 [13] M.-H. Yung and A. Aspuru-Guzik, *Proc. Natl. Acad. Sci. USA* **109**, 754 (2012).  
 [14] M. Motta, C. Sun, A. T. Tan, M. J. O’Rourke, E. Ye, A. J. Minnich, F. G. Brandão, and G. K.-L. Chan, *Nat. Phys.* **16**, 205 (2020).  
 [15] S.-N. Sun, M. Motta, R. N. Tazhigulov, A. T. K. Tan, Garnet Kin-Lic Chan, and A. J. Minnich, *PRX Quantum* **2**, 010317 (2021).  
 [16] S. Sugiura and A. Shimizu, *Phys. Rev. Lett.* **108**, 240401 (2012).  
 [17] S. Sugiura and A. Shimizu, *Phys. Rev. Lett.* **111**, 010401 (2013).  
 [18] L. Coopmans, Y. Kikuchi, and M. Benedetti, *PRX Quantum* **4**, 010305 (2023).  
 [19] C. Powers, L. B. Otfelie, and D. Camps, and W. A. de Jong, *Sci. Rep.* **13**, 1986 (2023).  
 [20] M. Suzuki, *Phys. Lett. A* **146**, 319 (1990).  
 [21] J. M. Martyn, Z. M. Rossi, A. K. Tan, and I. L. Chuang, *PRX Quantum* **2**, 040203 (2021).  
 [22] Y. Yamaji, T. Suzuki, T. Yamada, S.-i. Suga, N. Kawashima, and M. Imada, *Phys. Rev. B* **93**, 174425 (2016).  
 [23] H. Endo, C. Hotta, and A. Shimizu, *Phys. Rev. Lett.* **121**, 220601 (2018).  
 [24] T. Suzuki and Y. Yamaji, *J. Phys. Soc. Jpn.* **88**, 115001 (2019).  
 [25] R. Schäfer, I. Hagymási, R. Moessner, and D. J. Luitz, *Phys. Rev. B* **102**, 054408 (2020).  
 [26] T. Shimokawa, *Phys. Rev. B* **103**, 134419 (2021).  
 [27] H. Tomishige, J. Nasu, and A. Koga, *Phys. Rev. B* **97**, 094403 (2018).  
 [28] A. Koga, S. Nakauchi, and J. Nasu, *Phys. Rev. B* **97**, 094427 (2018).

- [29] A. Koga, H. Tomishige, and J. Nasu, *J. Phys. Soc. Jpn.* **87**, 063703 (2018).
- [30] J. Oitmaa, A. Koga, and R. R. P. Singh, *Phys. Rev. B* **98**, 214404 (2018).
- [31] A. Koga and J. Nasu, *Phys. Rev. B* **100**, 100404(R) (2019).
- [32] C. Hickey and S. Trebst, *Nat. Commun.* **10**, 530 (2019).
- [33] K. Morita and T. Tohyama, *Phys. Rev. Res.* **2**, 013205 (2020).
- [34] H. Taguchi, Y. Murakami, and A. Koga, *Phys. Rev. B* **105**, 125137 (2022).
- [35] K. Seki and S. Yunoki, *Phys. Rev. B* **106**, 155111 (2022).
- [36] G. H. Low, T. J. Yoder, and I. L. Chuang, *Phys. Rev. X* **6**, 041067 (2016).
- [37] A. Gilyén, Y. Su, G. H. Low, and N. Wiebe, [arXiv:1806.01838](https://arxiv.org/abs/1806.01838).
- [38] G. H. Low and I. L. Chuang, *Quantum* **3**, 163 (2019).
- [39] A. M. Childs and N. Wiebe, *Quantum Inf. Comput.* **12**, 901 (2012).
- [40] G. H. Low and I. L. Chuang, [arXiv:1707.05391](https://arxiv.org/abs/1707.05391).
- [41] S. Aaronson and D. Gottesman, *Phys. Rev. A* **70**, 052328 (2004).
- [42] X.-M. Zhang, T. Li, and X. Yuan, *Phys. Rev. Lett.* **129**, 230504 (2022).
- [43] G. H. Low and I. L. Chuang, *Phys. Rev. Lett.* **118**, 010501 (2017).
- [44] L. K. Grover, *STOC '96: Proceedings of the twenty-eighth annual ACM symposium on Theory of Computing* (Association for Computing Machinery, New York, 1996), pp. 212–219.
- [45] A. Peruzzo, J. McClean, P. Shadbolt, M.-H. Yung, X.-Q. Zhou, P. J. Love, A. Aspuru-Guzik, and J. L. O'Brien, *Nat. Commun.* **5**, 4213 (2014).
- [46] E. Farhi, J. Goldstone, S. Gutmann, and M. Sipser, [arXiv:quant-ph/0001106](https://arxiv.org/abs/quant-ph/0001106).
- [47] L. Lin and Y. Tong, *Quantum* **4**, 372 (2020).
- [48] Y. Dong, L. Lin, and Y. Tong, *PRX Quantum* **3**, 040305 (2022).
- [49] W. Kirby, M. Motta, and A. Mezzacapo, *Quantum* **7**, 1018 (2023).
- [50] N. H. Stair, R. Huang, and F. A. Evangelista, *J. Chem. Theory Comput.* **16**, 2236 (2020).
- [51] C. L. Cortes and S. K. Gray, *Phys. Rev. A* **105**, 022417 (2022).
- [52] N. H. Stair, C. L. Cortes, R. M. Parrish, J. Cohn, and M. Motta, *Phys. Rev. A* **107**, 032414 (2023).
- [53] Y. Yoneta and A. Shimizu, *Phys. Rev. B* **99**, 144105 (2019).
- [54] F. Jin, D. Willsch, M. Willsch, H. Lagemann, K. Michielsen, and H. De Raedt, *J. Phys. Soc. Jpn.* **90**, 012001 (2021).
- [55] A. Kitaev, *Ann. Phys.* **321**, 2 (2006).